JACS
JOURNAL OF THE AMERICAN CHEMICAL SOCIETY
pubs.acs.org/JACS
Article

Chemically Triggered Coalescence and Reactivity of Droplet Fibers

Jing Zhao, Zehao Pan, Deborah Snyder, Howard A. Stone, and Todd Emrick*

Cite This: J. Am. Chem. Soc. 2021, 143, 5558−5564
Read Online
ACCESS | Metrics & More | Article Recommendations | Supporting Information

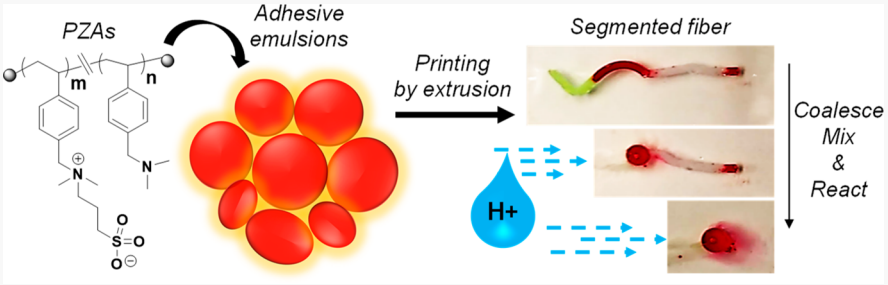

ABSTRACT: We describe the role of functional polymer surfactants in the construction and triggered collapse of droplet-based fibers and the use of these macroscopic supracolloidal structures for reagent compartmentalization. Copolymer surfactants containing both zwitterionic and tertiary amine pendent groups were synthesized for stabilization of oil-in-water droplets, in which the self-adherent properties of the selected zwitterions impart interdroplet adherence, while the amine groups provide access to pH-triggered coalescence. Macroscopic fibers, obtained by droplet extrusion, were prepared with reagents embedded in spatially distinct components of the fibers. Upon acidification of the continuous aqueous phase, protonation of the polymer surfactants increases their hydrophilicity and causes rapid fiber disruption and collapse. Cross-linked versions of these supracolloidal fibers were stable upon acidification and appeared to direct interdroplet passage of encapsulants along the fiber length. Overall, these functional, responsive emulsions provide a strategy to impart on-demand chemical reactivity to soft materials structures that benefits from the interfacial chemistry of the system.

INTRODUCTION

Polymer-stabilized emulsion droplets are long-studied and have a wide range of ongoing and emerging applications that span industrial and consumer products, personal care, and delivery systems.[1] As "soft solids", emulsions create opportunities for assembly into structures with tunable rheological properties.[2] The interdroplet interactions necessary for structure formation arising from functional surfactants at the fluid−fluid interface may involve H-bonding,[3−5] electrostatics,[6] or other modes of noncovalent connection.[7−9] However, many of these assembly methods are irreversible, or practically so, such that new discoveries are needed whereby weak, collective chemical interactions are employed strategically in macrostructure design. Such reversible assembly represents a balance between the initial stability required for structure generation and control over emulsion disruption by employing pH,[10−12] temperature,[13,14] light,[15] or other stimuli. Microfluidic designs represent one method for controlling droplet contact and driving coalescence by application of force (mechanical,[16,17] electrical,[18,19] or chemical[20]) but are limited by their relatively sophisticated designs and scale-up challenges.

In this paper we describe multifunctional polymers at fluid−fluid interfaces that provide new routes to chemically triggered droplet coalescence and collapse of soft solids in fluidic environments. The interfacial properties of the polymers utilized hinge on the presence of hydrophilic groups, in the form of zwitterions and amines, strung along a hydrophobic polymer backbone. While zwitterion-stabilized emulsions and mixed small molecule interfacial assemblies have been reported,[21−23] polymer approaches are advantageously versatile as they offer tunable extents of functionality and molecular weights that tailor fluid−fluid interactions. In our system, structural responses to solution stimuli are dictated by the selected sulfobetaine zwitterions, which are sensitive to ionic strength, and the tertiary amines, which are pH-responsive. This zwitterion/amine combination yielded fiber-like supracolloidal assemblies of polymer-stabilized droplets that functioned as multiresponsive macrostructures. Notably, a pH-triggered self-coalescence, based on altering the interfacial tension of the polymer, initiated reactions among reagents that were initially compartmentalized. Additional insight into interdroplet communication, enabled by the interfacial contact

Received: March 11, 2021
Published: April 1, 2021

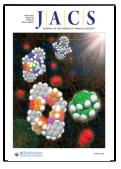

https://doi.org/10.1021/jacs.1c02576
J. Am. Chem. Soc. 2021, 143, 5558−5564

of "sticky droplets", is realized by using these responsive polymeric interfacial reagents.

RESULTS AND DISCUSSION

Polymer Synthesis and Fundamental Solution Properties. The polymeric zwitterionic/amine (**PZA**) copolymers illustrated in Figure 1 integrate both sulfobetaine (SB)

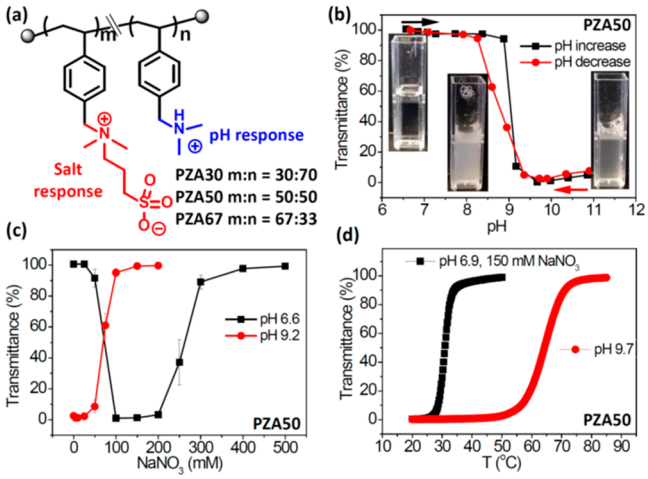

Figure 1. (a) Chemical structure of **PZA** copolymers containing both zwitterionic (Z) and amine (A) functionality. (b) Plot of transmittance as a function of pH for **PZA-50**. (c) Plot of transmittance as a function of [salt] at pH 6.6 and 9.2. (d) Plot of transmittance as a function of temperature at pH 6.9 with [salt] = 150 mM (black) and 9.7 (red). [Polymer] = 1 mg/mL in parts b–d.

zwitterions and tertiary amines (quaternary ammoniums) onto a polystyrene backbone. These copolymers were synthesized by reversible addition–fragmentation chain-transfer (RAFT) polymerization using 4-cyano-4-[(dodecylsulfanylthiocarbonyl)sulfanyl]pentanoic acid as the chain-transfer agent and 4,4′-azobis(4-cyanovaleric acid) (ACVA) as the free radical initiator.[24,25] Performing the polymerization in a water/2,2,2-trifluoroethanol (TFE) mixture at 70 °C contributed monomer and polymer solubility throughout the course of the polymerization. Continuing the polymerizations for ∼24 h produced >90% conversion of each monomer, with the polymer products having substantial molecular weights (∼40 kDa) and relatively narrow polydispersity index (PDI) values (∼1.1–1.2), as estimated by gel permeation chromatography (GPC). The polymers were isolated as white solids in gram quantities following dialysis and lyophilization, and the ratio of monomers integrated into the polymer products was judged by ^{1}H NMR spectroscopic integration of the benzylic SB and amine methylene groups at δ 4.5 and 4.2 ppm, respectively. The incorporated monomer ratios corresponded closely to the feed ratios employed, affording products with ∼30, 50, and 67 mol % SB groups, denoted **PZA-30**, **PZA-50**, and **PZA-67**, respectively. Figure S1 and Tables S1 and S2 summarize the characterization of these copolymers.

The fundamental solution properties of **PZA** polymers were probed by turbidity measurements as a function of pH, salt concentration, and temperature, with key characterization data given in Figures 1b–d for the example of **PZA-50**. At pH > 9, when the amines are neutral, the polymer solution appeared turbid due to insolubility of the SB component in salt-free water (Figure 1b).[24] Transmittance increased rapidly with amine protonation as the solution was acidified, with an abrupt change at pH ∼ 9, while the SB-zwitterions were unaffected across the investigated pH range (a conductivity titration measurement showed a similarly abrupt transition in this pH range (Figure S2)). Copolymer solution behavior in salt water proved more complex, since salt simultaneously impacts electrostatic screening of both the zwitterions and amines, by (1) disrupting inter-zwitterion interactions[24−27] (to increase solubility) and (2) screening charge repulsion[28] (to decrease solubility) (Figure 1c). At pH 9.2, where the polymer is charge-neutral, turbidity measurements suggested "anti-polyelectrolyte" behavior typical of SB-polymers,[24] characterized by insolubility at very low salt concentration and rapidly increasing solubility at >50 mM salt. This behavior contrasted with the more complex behavior of **PZA-50** at pH 6.6, when the amines are protonated, where solubility at low salt concentration was lost at higher concentrations, a "salting-out" effect resulting from polyelectrolyte screening and hydrophobic interactions. However, for the same polymer, further increasing salt concentration to 300 mM recaptures clean solution transmittance as the polymer is "salted-in", since at this stage the SB-zwitterion component dominates solution behavior. Such a U-shaped optical transmission curve qualitatively resembles examples of charge-unbalanced polyampholytes (i.e., with positive and negative charges on separate monomer units),[29] though we are not aware of related findings for polymer zwitterions. Similar solution studies performed by using **PZA-30** and **PZA-67** showed excellent control over the impact of solution properties on structure by adjusting the SB-to-amine ratio. In accord with this rationale, polymers with lower SB percentages required higher salt concentration to achieve transparent solutions (Figure S3b); this is reflected in the transmittance data for samples studied under acidic conditions, in which transitions to optical clarity shifted to higher salt concentration for polymers with lower SB content (Figure S3c). Notably, the U-shaped curve describing salt response depended on salt composition, as presented in Figure S4 for **PZA-50**. Within the conventional Hofmeister series,[30,31] salts to the right of $NaNO_3$ (e.g., NaBr and NaI) produced U-shaped transmittance, while those to the left (e.g., NaCl, sodium acetate, and Na_2SO_4) solubilized **PZA-50** across the entire concentration range.

Combining copolymer protonation levels with temperature afforded further control over solution transitions, as shown in Figure 1d. At pH 6.9 and 150 mM $NaNO_3$(aq), room temperature insolubility quickly yielded to a transparent solution at >35 °C; in contrast, with neutral amines at pH 9.7, the cloud point was ∼30 °C higher. Irrespective of amine protonation, salt-induced interruption of inter-zwitterionic interactions reduced the cloud point well below that of the SB-based homopolymer (25% transmittance at 90 °C). Preliminary evidence for additional interesting phase behavior of these zwitterion/cationic macromolecules is shown in Figure S5, in which an apparent liquid–liquid phase separation in water produces micrometer-sized structures that resemble polymer-based coacervates, structures that typically result from combining oppositely charged polyelectrolytes at high salt concentration.[32]

PZA-Induced Droplet Adhesion and Triggered Transitions. The fundamental solution properties described above were used to underpin our study of macrostructures built from **PZA**-stabilized droplets. Figure 2a shows pendant drop tensiometry measurements of **PZA-50** at the oil–water

https://doi.org/10.1021/jacs.1c02576
J. Am. Chem. Soc. 2021, 143, 5558−5564

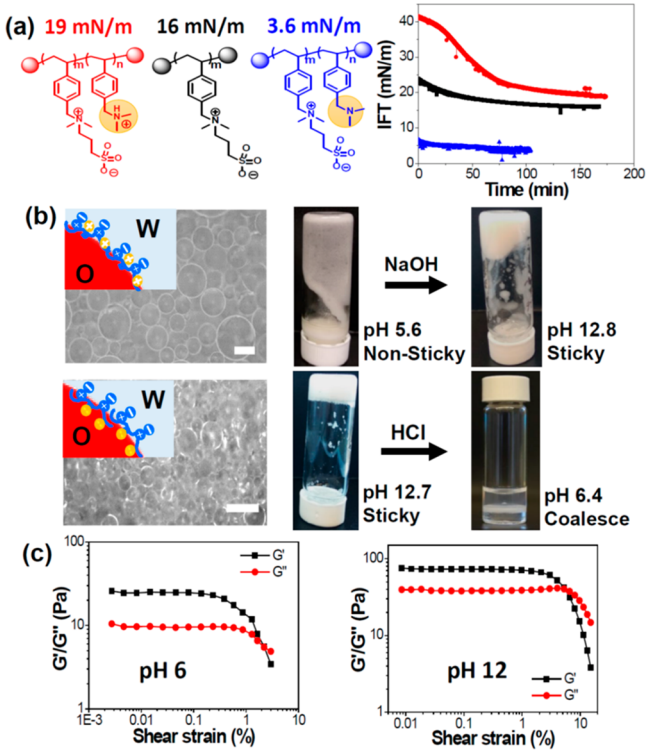

Figure 2. (a) **PZA-50** (red and blue), SB-substituted polystyrene, and their measured interfacial tension (IFT) values. (b) Schematic illustration, optical micrographs, and photographs of emulsions stabilized by **PZA-50** (scale bars = 100 μm). (c) Viscoelasticity of **PZA-50** as a function of the oscillatory shear strain at a fixed frequency of 10 rad/s. [Polymer] = 10 mg/mL; oil = TCB; oil phase fraction (φ_{oil}) = 0.63 (pH 6.4) and (φ_{oil}) = 0.67 (pH 9.6).

interface (oil = trichlorobenzene (TCB)), in which the neutral polymer produces a much larger reduction in interfacial tension (σ = 3.6 mN/m) relative to the more hydrophilic polyelectrolyte (σ = 19.0 mN/m), which is shown in Table S3. While both the neutral and cationic forms of **PZA-50** stabilized oil-in-water droplets, such modulation of pH-induced interfacial tension allowed on-demand transition from self-adhesive (neutral polymer surfactant) to nonadhesive (cationic surfactant) droplets (Figure S6 provides data for the range of polymers studied). Typically, **PZA**-stabilized droplets were prepared by vortexing (1200 rpm for ∼1 min) a mixture of oil (e.g., TCB), water, and polymer (∼10 mg/mL). Optical microscopy images (Figure 2b) confirmed the formation of spherical droplets, 50−200 μm in diameter, formed at pH 6, with stability aided by electrostatic repulsion of the cationic component. At pH 12, the droplets were smaller (10−100 μm diameter) and clustered into dense piles, an indication of apparent interdroplet adhesion that has macroscopic implications for structure formation and interdroplet communication (*vide infra*). Importantly, the surfactant properties of **PZA-50** persisted over a wide pH range, in contrast to the narrow pH window associated with numerous responsive polymer surfactants.[10−12]

Emulsion droplets stabilized by **PZA-50** appear nonadhesive at low pH due to electrostatic repulsion from the cationic component but adhesive when the amines are neutral, where hydrophobic and inter-SB interactions dominate droplet behavior (Figure S6). Notably, the zwitterion-to-amine ratio determined interfacial behavior, seen for example in **PZA-30**, in which droplets coalesced at low pH, since the relatively low zwitterion content could not maintain sufficient surfactant properties. For **PZA-50**, the nonadhesive-to-adhesive transition evident in Figure 2b hinges on the amine protonation state: a flowing emulsion in a glass vial turned visibly sticky upon addition of base, with markedly larger interdroplet contact angles reflecting stickiness (Figure S7b). Rheological measurements of these emulsions were performed by using a stress-controlled rheometer equipped with a parallel plate geometry (plate diameter of 50 mm) and an arithmetic average roughness (R_a) of the plates of 6−7 μm to minimize wall slip. The rheology results reflected our visual observations: about 3 times greater elastic modulus (G') and 4 times greater viscous modulus (G'') were seen for the sticky emulsions, with a corresponding increase in crossover shear strain (Figure 2c). Interestingly, for **PZA-30** and **PZA-50**, acidifying the sticky emulsions resulted in rapid droplet coalescence rather than droplet dispersion (Figure 2b and Figure S6c). This is likely due to the large interfacial tension change upon polymer protonation (∼15 mN/m for **PZA-50**) and the associated changes in pressure (proportional to interfacial tension) in the Plateau borders of the droplets.[33,34] In sharp contrast, for **PZA-67**-stabilized droplets, acidifying the adhesive emulsion resulted in clean droplet dispersion rather than coalescence (Figure S6c) because of the high zwitterionic content that dominates fluid−fluid interfacial interactions and leads to a smaller interfacial tension change (∼6 mN/m).

The U-shaped transmittance vs salt concentration profile seen for **PZA-50** (Figure 1c) translated to the observed droplet properties. For droplets prepared under acidic conditions, a distinct transition of *nonsticky to sticky to nonsticky* (Figures S8a and S9b) was observed, in agreement with polymer solubility trends. This finding is particularly interesting, since reversing the first transition does not require dilution with large volumes of fluid. Likewise, the thermal solution properties of the copolymers proved impactful on droplet interfaces—at both high and low pH, heating sticky emulsions above the cloud point of their constituent polymers caused "melting" of the emulsion constructs and allowed remolding or reconfiguration of a given droplet structure (Figures S8c and S9c). These reconfigurations occurred smoothly, suggesting excellent thermal and salt stability of **PZA-50**-stabilized droplets and the potential for building reconfigurable structures from them. It is worth noting that these findings bear a conceptual relationship to recently described systems exhibiting "reentrant gelation",[35,36] in which stimulus (usually temperature) effects a gel to sol to gel transition.

PZA Droplet Macrostructures—Preparation and Reagent Compartmentalization. The pH-induced fluidic-to-adhesive transition of **PZA-50**-stabilized droplets makes them uniquely suited for printing soft structures, confining reagents, and enabling transport along a supracolloidal pathway. As seen in Figure 3a, attempts to print droplets from nonsticky (pH 7) conditions failed to produce robust structures, whereas printing the droplets into a basic solution produced structures that maintained their shape even upon agitation of the water. Interestingly, extrusion of droplets in an already sticky state (i.e., starting from basic conditions) into aqueous base afforded gels containing discrete, observable fibers but lacking fiber-to-fiber adhesion and therefore rupturing into smaller fibers upon agitation. **PZA-50** droplets were also amenable to vertical construction, shown in the towers in Figure 3b, in which the injected droplets assumed the

https://doi.org/10.1021/jacs.1c02576
J. Am. Chem. Soc. 2021, 143, 5558−5564

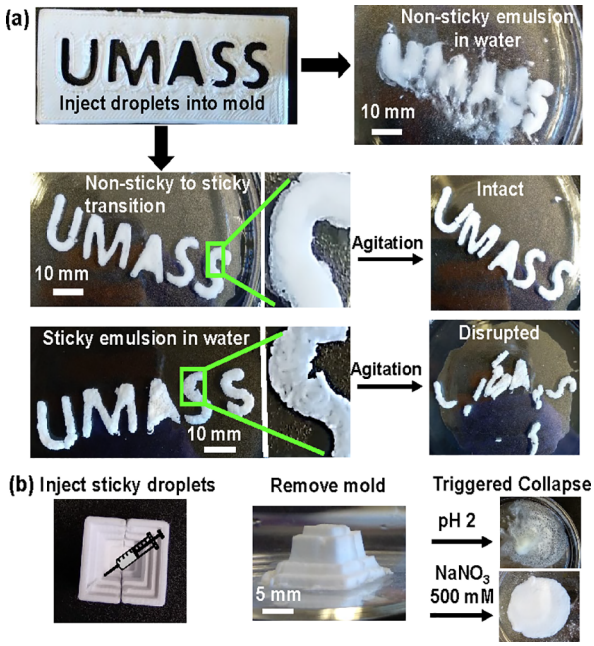

Figure 3. Photographs of emulsion-based gels assembled from **PZA-50**-stabilized droplets. (a) Plastic UMASS mold filled with oil droplets in water: nonsticky emulsion injected into water (top) and sticky emulsion injected into aqueous base and then agitated (bottom). (b) Vertical assembly of emulsion droplet towers and disassembly by contact with aqueous acid or salt water. [Polymer] = 10 mg/mL; oil = TCB; oil phase fraction (φ_{oil}) of nonsticky emulsion (φ_{oil}) = 0.63 (pH = 6.4); for sticky emulsion, φ_{oil} = 0.67 (pH = 9.6).

shape of the plastic container and maintained that shape following removal of the mold, benefiting from preferable interdroplet interactions over adhesion to the plastic walls. Notably, these emulsion gels formed instantly and did not require additives to maintain their structures.[37] The towers stood in water for 1 day without noticeable change and remained stable until contacting aqueous acid or salt solutions (e.g., 500 mM $NaNO_3$) that caused them to "melt" by coalescence (from acid) or droplet dispersion (from salt water).

To prepare multisegment droplet fibers, sequential stacking of adhesive droplets in a capillary tube (i.d. ~ 1500 μm) was followed by gentle extrusion into water by applying pressure through an inserted needle.[38] This allowed for compartmentalization of encapsulated components (e.g., dyes, reagents, nanoparticles, etc.) within predefined segments spaced along the length of the fiber, which was maintained after extrusion, as shown in Figure 4. The amines of **PZAs** gave access to pH-triggered fiber coalescence, whereby addition of aqueous acid to the yellow end of the fiber in Figure 4a led to its rapid (~30 s) and complete conversion into one (or a few) large droplet(s) (see Movie S1 for visualization of triggered coalescence). The fluorescence of the fluid interface after coalescence (seen in experiments employing FITC-labeled **PZA-50**) suggests that the protonated **PZA** ultimately stabilizes the fluid–fluid interface after fiber coalescence (Figure S10).

We note that a similarly triggered fiber coalescence was observed when organic acids, such as gluconic or acetic acid, were added to the aqueous phase or generated *in situ*. Therefore, inspired by enzyme micropumps described by Sen and Balazs,[39−41] we tested whether enzymatic reactions

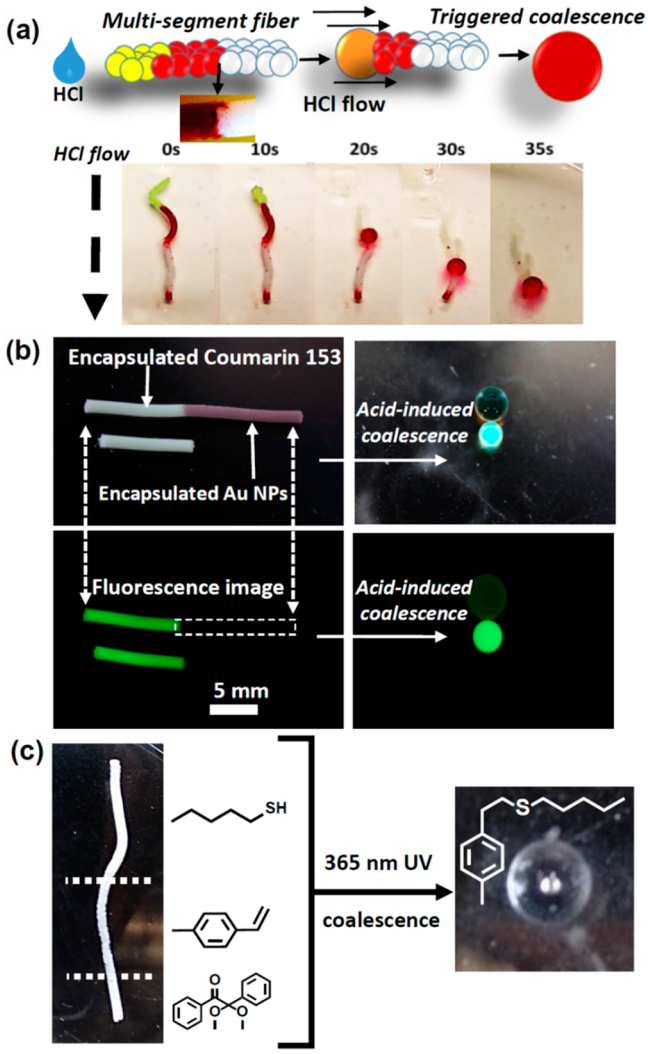

Figure 4. (a) Self-coalescence of multisegment supracolloidal fiber. (b) Fluorescence quenching in a two-segment fiber. (c) Thiol–ene addition following collapse of a three-segment fiber. Experimental conditions: in (a–c), [polymer] = 10 mg/mL; in (a), the oil phase = TCB with 1 mg/mL Dispersed Red 13 or 1 mg/mL Coumarin 153; in (b), the oil phase is TCB with 0.1 mg/mL Coumarin 153 or 0.5 mg/mL Au NPs; in (c), the oil phase is α,α,α-trifluorotoluene (1.14 M 1-pentanethiol; 0.76 M 4-methylstyrene; 0.76 M DMPA).

occurring in the vicinity of the fiber could be utilized to trigger droplet coalescence and fiber collapse. This was done by immobilizing glucose oxidase (GOx) to an Au-patterned Si wafer via a quaternary ammonium-terminated self-assembled monolayer, as illustrated in Figures S11 and S12. Addition of D-glucose (20 mg/mL) to the aqueous solution of these enzyme-containing systems (producing gluconic acid and hydrogen peroxide) led to slow fiber coalescence over a 24 h period, while control experiments lacking the immobilized enzyme caused no change in fiber morphology (Figure S13).

In principle, the triggered self-coalescence that we describe is useful for designing multisegment microreactors, which we demonstrate for reagents encapsulated in the droplet constituents of **PZA-50**-stabilized fibers. For example, a fiber in water with distinct segments of dye (Coumarin 153) and Au NPs, each encapsulated in oil-in-water emulsion droplets (oil = TCB), collapses after addition of acid (Figure 4b). Coalescence-induced mixing of these components quenched

https://doi.org/10.1021/jacs.1c02576
J. Am. Chem. Soc. 2021, 143, 5558−5564

the dye's fluorescence, whereas in the dye-only experiment, fluorescence and efficient dye encapsulation were maintained following coalescence. In similar fashion, a three-segment droplet fiber was prepared, in which the segments contained 4-methylstyrene, 1-pentanethiol, and 2,2-dimethoxy-2-phenylacetophenone segments (Figure 4c). Triggering fiber collapse caused reagent mixing and UV-induced thiol−ene addition, as confirmed by ^{1}H NMR spectroscopy of the collected oil phase (Figure S14). Notably, despite close contact of the droplets within these fibers, reagent mixing prior to collapse is negligible over this time frame, as confirmed by a control experiment in which the three-segment fiber was subjected to UV irradiation prior to coalescence, resulting in no observable sulfide product.

Functional versions of **PZA**-stabilized fibers offer versatility in their performance, as seen in UV-cross-linked fibers (enabled by integration of benzophenone methacrylamide into the **PZA** polymer), in which chemical cross-linking prevented droplet coalescence such that the fibers resisted collapse when in contact with aqueous acid (Figure 5 and Figure S15). The cross-linked fibers proved stable for weeks or longer under acidic conditions and fluorescence confocal microscopy images (Figure 5a) produced similar images of fluorescent droplets along the fiber length at both pH 2 and pH 12. Photobleaching of the fiber (via confocal microscopy, Figure S16) confirmed the expected lack of polymer mobility following cross-linking, in contrast to rapid fluorescence recovery for individual (un-cross-linked) **PZA 50**-stabilized droplets. As shown in Figure 5b, a cross-linked fiber immersed in water was connected to an oil droplet by injecting the droplet onto the fiber end with a blunt needle. Interestingly, cross-linked fibers containing this droplet reservoir showed evidence of dye transport (Figure 5c) along the length of the fiber, over the course of days, which we suggest to occur via direct transport of dye among interconnected droplets, along the Plateau borders, rather than by micelle-mediated transport.[42,43] This dye transport was induced by acidifying the liquid medium surrounding the fiber, ultimately generating a fiber with visible dye along the entire length at pH 2, whereas almost no transport was visible at pH 7 and above. Similar results were seen for two-component fibers, in which the organic dye was segregated initially to droplets in one part of the fiber and then spread throughout the fiber over time (Figure S17). We speculate that protonation of the interfacial PZA stabilizer under acidic conditions may alter the interfacial structure and produce channels to allow such interdroplet transport, though confirming this will require detailed structural probing of interfacial structure in future work.

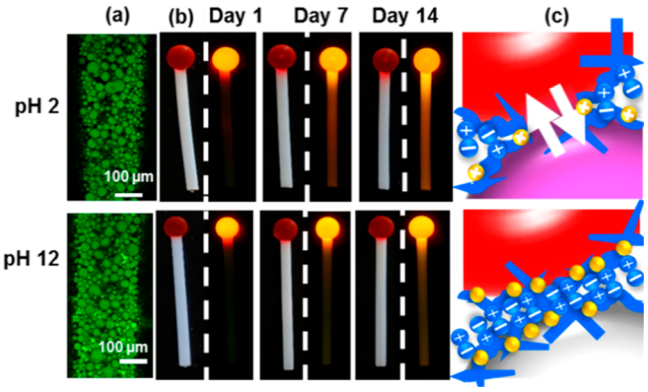

Figure 5. pH-induced interdroplet dye transport in cross-linked supracolloidal fibers at pH 2 (top row) and 12 (bottom row). (a) Z-slice from fluorescence confocal micrographs (emission 525 nm; excitation 488 nm). (b) Photographs (left) and fluorescence images (right) of **PZA**-stabilized droplet fibers immersed in water with a drop of dye-containing oil at the end. (c) Schematic illustration of pH-induced interfacial structural change leading to interdroplet transport. Conditions: [polymer] = 10 mg/mL; oil = TCB with Nile Red (1 mg/mL for (a) and 0.5 mg/mL for (b)).

CONCLUSION

In summary, we have described the preparation of novel, multiresponsive polymer surfactants by RAFT polymerization that incorporate both zwitterionic and tertiary amine pendent groups onto a polystyrene backbone. Emulsion droplets stabilized by these polymers ranged from self-adhesive to self-coalescing, depending on the extent of zwitterionic vs amine functionality, the selected solution conditions and triggers, and whether cross-linking chemistry was employed. By tuning these interactions, we shaped emulsions into supracolloidal structures by simple extrusion or printing techniques; multisegment versions of these fibers afforded spatial and temporal control over reactions, in which reagents remained separated prior to triggered fiber coalescence. Taken together, these responsive emulsions represent a new design strategy to fabricate smart, functional soft materials for any of a variety of applications involving functional, printable, soft material encapsulants.

ASSOCIATED CONTENT

Supporting Information

The Supporting Information is available free of charge at https://pubs.acs.org/doi/10.1021/jacs.1c02576.

Experimental section (section S1) with procedures and spectroscopic characterization (PDF)

Movie S1 (AVI)

AUTHOR INFORMATION

Corresponding Author

Todd Emrick − *Polymer Science & Engineering Department, University of Massachusetts Amherst, Amherst, Massachusetts 01003, United States;* orcid.org/0000-0003-0460-1797; Email: tsemrick@mail.pse.umass.edu

Authors

Jing Zhao − *Polymer Science & Engineering Department, University of Massachusetts Amherst, Amherst, Massachusetts 01003, United States*

Zehao Pan − *Department of Mechanical and Aerospace Engineering, Princeton University, Princeton, New Jersey 08544, United States*

Deborah Snyder − *Polymer Science & Engineering Department, University of Massachusetts Amherst, Amherst, Massachusetts 01003, United States*

Howard A. Stone − *Department of Mechanical and Aerospace Engineering, Princeton University, Princeton, New Jersey 08544, United States;* orcid.org/0000-0002-9670-0639

Complete contact information is available at: https://pubs.acs.org/10.1021/jacs.1c02576

Notes

The authors declare no competing financial interest.

■ ACKNOWLEDGMENTS

The authors acknowledge funding for this research from the National Science Foundation Center for Chemomechanical Assembly (NSF-CCI-1740630), an NSF-supported Phase I Center for Chemical Innovation (CCI). D.S. acknowledges support from the National Institutes of Health Biotechnology Training Program (1 T32 GM135096). We thank Dr. James Chambers for helpful discussions associated with microscopy data gathered in the Light Microscopy Facility and Nikon Center of Excellence at the Institute for Applied Life Sciences (IALS) at UMass Amherst, with support from the Massachusetts Life Sciences Center.

■ REFERENCES

(1) Chappat, M. Some Applications of Emulsions. *Colloids Surf., A* **1994**, *91* (3), 57−77.
(2) Kim, H. S.; Mason, T. G. Advances and Challenges in the Rheology of Concentrated Emulsions and Nanoemulsions. *Adv. Colloid Interface Sci.* **2017**, *247*, 397−412.
(3) Weaver, J. V. M.; Rannard, S. P.; Cooper, A. I. Polymer-Mediated Hierarchical and Reversible Emulsion Droplet Assembly. *Angew. Chem., Int. Ed.* **2009**, *48* (12), 2131−2134.
(4) Woodward, R. T.; Weaver, J. V. M. The Role of Responsive Branched Copolymer Composition in Controlling pH-Triggered Aggregation of "Engineered" Emulsion Droplets: Towards Selective Droplet Assembly. *Polym. Chem.* **2011**, *2* (2), 403−410.
(5) Woodward, R. T.; Chen, L.; Adams, D. J.; Weaver, J. V. M. Fabrication of Large Volume, Macroscopically Defined and Responsive Engineered Emulsions Using a Homogeneous pH-Trigger. *J. Mater. Chem.* **2010**, *20* (25), 5228−5234.
(6) Maçon, A. L. B.; Rehman, S. U.; Bell, R. V.; Weaver, J. V. M. Reversible Assembly of pH Responsive Branched Copolymer-Stabilised Emulsion via Electrostatic Forces. *Chem. Commun.* **2016**, *52* (1), 136−139.
(7) Villar, G.; Graham, A. D.; Bayley, H. A Tissue-Like Printed Material. *Science* **2013**, *340* (6128), 48−52.
(8) Xu, J.; Sigworth, F. J.; LaVan, D. A. Synthetic Protocells to Mimic and Test Cell Function. *Adv. Mater.* **2010**, *22* (1), 120−127.
(9) Poulin, P.; Bibette, J. Adhesion of Water Droplets in Organic Solvent. *Langmuir* **1998**, *14* (22), 6341−6343.
(10) Xu, P.; Wang, Z.; Xu, Z.; Hao, J.; Sun, D. Highly Effective Emulsification/Demulsification with a CO_2-Switchable Superamphiphile. *J. Colloid Interface Sci.* **2016**, *480*, 198−204.
(11) Lu, Y.; Sun, D.; Ralston, J.; Liu, Q.; Xu, Z. CO_2-Responsive Surfactants with Tunable Switching pH. *J. Colloid Interface Sci.* **2019**, *557*, 185−195.
(12) Liu, Y.; Jessop, P. G.; Cunningham, M.; Eckert, C. A.; Liotta, C. L. Switchable Surfactants. *Science* **2006**, *313* (5789), 958−960.
(13) Hiranphinyophat, S.; Asaumi, Y.; Fujii, S.; Iwasaki, Y. Surface Grafting Polyphosphoesters on Cellulose Nanocrystals to Improve the Emulsification Efficacy. *Langmuir* **2019**, *35* (35), 11443−11451.
(14) Feng, H.; Verstappen, N. A. L.; Kuehne, A. J. C.; Sprakel, J. Well-Defined Temperature-Sensitive Surfactants for Controlled Emulsion Coalescence. *Polym. Chem.* **2013**, *4* (6), 1842−1847.
(15) Dixit, S. S.; Kim, H.; Vasilyev, A.; Eid, A.; Faris, G. E. Light-Driven Formation and Rupture of Droplet Bilayers. *Langmuir* **2010**, *26* (9), 6193−6200.
(16) Liu, M.; Cao, X.; Zhu, Y.; Guo, Z.; Zhang, L.; Zhang, L.; Zhao, S. The Effect of Demulsifier on the Stability of Liquid Droplets: A Study of Micro-Force Balance. *J. Mol. Liq.* **2019**, *275*, 157−162.
(17) Pawar, A. B.; Caggioni, M.; Ergun, R.; Hartel, R. W.; Spicer, P. T. Arrested Coalescence in Pickering Emulsions. *Soft Matter* **2011**, *7* (17), 7710−7716.
(18) Thiam, A. R.; Bremond, N.; Bibette. Adhesive Emulsion Bilayers under an Electric Field: From Unzipping to Fusion. *Phys. Rev. Lett.* **2011**, *107* (6), 068301.
(19) Rozynek, Z.; Mikkelsen, A.; Dommersnes, P.; Fossum, J. O. Electroformation of Janus and Patchy Capsules. *Nat. Commun.* **2014**, *5*, 3945.
(20) Thiam, A. R.; Bremond, N.; Bibette, J. From Stability to Permeability of Adhesive Emulsion Bilayers. *Langmuir* **2012**, *28* (15), 6291−6298.
(21) Danov, K. D.; Kralchevska, S. D.; Kralchevsky, P. A.; Ananthapadmanabhan, K. P.; Lips, A. Mixed Solutions of Anionic and Zwitterionic Surfactant (Betaine): Surface-Tension Isotherms, Adsorption, and Relaxation Kinetics. *Langmuir* **2004**, *20* (13), 5445−5453.
(22) Seredyuk, V.; Alami, E.; Nydén, M.; Holmberg, K.; Peresypkin, A. V.; Menger, F. M. Micellization and Adsorption Properties of Novel Zwitterionic Surfactants. *Langmuir* **2001**, *17* (17), 5160−5165.
(23) Zhang, Q.; Cai, B.; Gang, H.; Yang, S.; Mu, B. A Family of Novel Bio-Based Zwitterionic Surfactants Derived from Oleic Acid. *RSC Adv.* **2014**, *4*, 38393−38396.
(24) Letteri, R. A.; Santa Chalarca, C. F.; Bai, Y.; Hayward, R. C.; Emrick, T. Forming Sticky Droplets from Slippery Polymer Zwitterions. *Adv. Mater.* **2017**, *29* (38), 1702921.
(25) Santa Chalarca, C. F.; Letteri, R. A.; Perazzo, A.; Stone, H. A.; Emrick, T. Building Supracolloidal Fibers from Zwitterion-Stabilized Adhesive Emulsions. *Adv. Funct. Mater.* **2018**, *28* (45), 1804325.
(26) Huang, K.; Ishihara, K.; Huang, C. Polyelectrolyte and Antipolyelectrolyte Effects for Dual Salt-Responsive Interpenetrating Network Hydrogels. *Biomacromolecules* **2019**, *20* (9), 3524−3534.
(27) Ilčíková, M.; Tkáč, J.; Kasák, P. Switchable Materials Containing Polyzwitterion Moieties. *Polymers* **2015**, *7* (11), 2344−2370.
(28) Curtis, K. A.; Miller, D.; Millard, P.; Basu, S.; Horkay, F.; Chandran, P. L. Unusual Salt and pH Induced Changes in Polyethylenimine Solutions. *PLoS One* **2016**, *11* (9), e0158147.
(29) Zhao, J.; Burke, N. A. D.; Stöver, H. D. H. Preparation and Study of Multi-Responsive Polyampholyte Copolymers of *N*-(3-aminopropyl) methacrylamide hydrochloride and Acrylic acid. *RSC Adv.* **2016**, *6* (47), 41522−41531.
(30) Kunz, W.; Henle, J.; Ninham, B. W. 'Zur Lehre von der Wirkung der Salze' (about the Science of the Effect of Salts): Franz Hofmeister's Historical Papers. *Curr. Opin. Colloid Interface Sci.* **2004**, *9* (1−2), 19−37.
(31) Delgado, J. D.; Schlenoff, J. B. Static and Dynamic Solution Behavior of a Polyzwitterion Using a Hofmeister Salt Series. *Macromolecules* **2017**, *50* (11), 4454−4464.
(32) Liu, Y.; Momani, B.; Winter, H. H.; Perry, S. L. Rheological Characterization of Liquid-to-Solid Transitions in Bulk Polyelectrolyte Complexes. *Soft Matter* **2017**, *13* (40), 7332−7340.
(33) De Feijter, J. A; Rijnbout, J. B; Vrij, A Contact Angles in Thin Liquid Films. I. Thermodynamic Description. *J. Colloid Interface Sci.* **1978**, *64* (2), 258−268.
(34) Teixeira, P. I. C.; Fortes, M. A. Energy and Tension of Films and Plateau Borders in a Foam. *Colloids Surf., A* **2007**, *309* (1−3), 3−6.
(35) Tsujimoto, M.; Shibayama, M. Dynamic Light Scattering Study on Reentrant Sol−Gel Transition of Poly(vinyl alcohol)−Congo Red Complex in Aqueous Media. *Macromolecules* **2002**, *35* (4), 1342−1347.
(36) Shapira, R.; Katalan, S.; Edrei, R.; Eichen, Y. Chirality Dependent Inverse-Melting and Re-entrant Gelation in α-cyclodextrin/1-phenylethylamine Mixtures. *RSC Adv.* **2020**, *10*, 39195−39203.
(37) Zhang, Q.; Wang, C.; Fu, M.; Wang, J.; Zhu, S. Pickering High Internal Phase Emulsions Stabilized by Worm-Like Polymeric Nanoaggregates. *Polym. Chem.* **2017**, *8* (36), 5474−5480.
(38) Zhao, J.; Santa Chalarca, C. F.; Nunes, J. K.; Stone, H. A.; Emrick, T. Self-Propelled Supracolloidal Fibers from Multifunctional Polymer Surfactants and Droplets. *Macromol. Rapid Commun.* **2020**, *41* (15), 2000334.

https://doi.org/10.1021/jacs.1c02576
J. Am. Chem. Soc. 2021, 143, 5558−5564

(39) Sengupta, S.; Patra, D.; Ortiz-Rivera, O.; Agrawal, A.; Shklyaev, S.; Dey, K.; Cordova-Figueroa, U.; Mallouk, T.; Sen, A. Self-Powered Enzyme Micropumps. *Nat. Chem.* **2014**, *6* (5), 415−422.
(40) Shklyaev, O. E.; Shum, H.; Sen, A.; Balazs, A. C. Harnessing Surface-Bound Enzymatic Reactions to Organize Microcapsules in Solution. *Sci. Adv.* **2016**, *2* (3), e1501835.
(41) Maiti, S.; Shklyaev, O. E.; Balazs, A. C.; Sen, A. Self-Organization of Fluids in a Multienzymatic Pump System. *Langmuir* **2019**, *35* (10), 3724−3732.
(42) Meredith, C. H.; Moerman, P. G.; Groenewold, J.; Chiu, Y.; Kegel, W. K.; van Blaaderen, A.; Zarzar, L. D. Predator-Prey Interactions between Droplets Driven by Nonreciprocal Oil Exchange. *Nat. Chem.* **2020**, *12*, 1136−1142.
(43) Weiss, J.; Canceliere, C.; McClements, D. J. Mass Transport Phenomena in Oil-in-Water Emulsions Containing Surfactant Micelles: Ostwald Ripening. *Langmuir* **2000**, *16* (17), 6833−6838.

https://doi.org/10.1021/jacs.1c02576
J. Am. Chem. Soc. 2021, 143, 5558−5564